Life Sciences in Space Research 18 (2018) 64–71

Contents lists available at ScienceDirect

Life Sciences in Space Research

journal homepage: www.elsevier.com/locate/lssr

Comparison of space radiation GCR models to recent AMS data

John W. Norbury*,[a], Kathryn Whitman[b], Kerry Lee[b], Tony C. Slaba[a], Francis F. Badavi[c]

[a] NASA Langley Research Center, Hampton, Virginia 23681, USA
[b] NASA Johnson Space Center, Houston, Texas 77058, USA
[c] Old Dominion University, Norfolk, Virginia 23529, USA

ARTICLE INFO

Keywords:
Space radiation
Galactic cosmic rays
Alpha magnetic spectrometer

ABSTRACT

This paper is the third in a series of comparisons of American (NASA) and Russian (ROSCOSMOS) space radiation calculations. The present work focuses on calculation of fluxes of galactic cosmic rays (GCR), which are a constant source of radiation that constitutes one of the major hazards during deep space exploration missions for both astronauts/cosmonauts and hardware. In this work, commonly used GCR models are compared with recently published measurements of cosmic ray Hydrogen, Helium, and the Boron-to-Carbon ratio from the Alpha Magnetic Spectrometer (AMS). All of the models were developed and calibrated prior to the publication of the AMS data; therefore this an opportunity to validate the models against an independent data set.

1. Introduction

Plans are underway for further human exploration of deep space, beginning in the cis-lunar region with later expansion to Mars. Such large-scale exploration missions will continue to involve significant amounts of international cooperation. One of the major hazards for exploration of deep space is the harmful effects of space radiation on both astronauts/cosmonauts and electronic systems. A series of meetings has been taking place in Moscow, Russia between radiation experts from the space agencies of USA, Russia, Europe, Japan and Canada. Part of the aim of these meetings is to compare a wide variety of space radiation calculations and predictions, as well as to identify best-practice models and methods where possible. As a result of these meetings, two papers have already been published which compared flux calculations and pion cross section predictions from the American (NASA) and Russian (ROSCOSMOS) space radiation transport codes, HZETRN and SHIELD respectively (Norbury et al., 2017; 2018). The present work represents the third publication in this series which compares the galactic cosmic ray models used by NASA, ROSCOSMOS and the European Space Agency (ESA). The NASA GCR environment tool is the Badhwar-O'Neill model (O'Neill et al., 2015); the ROSCOSMOS tools are the International Standardization Organization ISO GCR model (Nymmik et al., 1992; 1994; 1996; International Standardization Organization ISO, 2004) and the new SINP (Skobeltsyn Institute of Nuclear Physics) model (Kuznetsov et al., 2017), while the ESA tool is the DLR (Deutsches zentrum für Luft- und Raumfahrt) model (Matthia et al., 2013). These models are compared to the most recent data available from the Alpha Magnetic Spectrometer (AMS) (Aguilar et al., 2015; 2015a; 2016) which is currently taking measurements from the International Space Station (ISS).

A variety of sensitivity studies have recently been performed to quantify the relative importance of specific ions and energies in the GCR spectrum to exposure behind shielding and tissue (Slaba and Blattnig, 2014, 2014a; Slaba et al., 2014), which included comparisons between NASA and DLR models to Advanced Composition Explorer / Cosmic Ray Isotope Spectrometer (ACE/CRIS), balloon data, and high energy PAMELA (Payload for Antimatter Matter Exploration and Light-nuclei Astrophysics) data (Slaba et al., 2014). The paper by Slaba et al. (2014) includes a detailed analysis of GCR model uncertainties. Highly efficient methods were developed to propagate GCR model uncertainty into exposure quantities behind shielding, and these efforts led to automated procedures that were subsequently used to refine GCR model parameters and significantly reduce uncertainties (O'Neill et al., 2015). (Obviously if a quantity is propagated through a material then the associated uncertainty must be propagated as well.) The same quantitative assessment tools were used to inform and define requirements for obtaining new and highly significant measurements from AMS. An important realization from these studies has been that 90% of the effective dose behind shielding is induced by GCR with energies above 500 MeV/n, which is the upper energy limit of the ACE/CRIS satellite that has contributed to most of the GCR measurement data. Clearly, higher energy data are needed, and that is why the AMS measurements are so important. Therefore, the present work focuses on comparisons to AMS measurements. The recommendation to compare various GCR models to high energy measurements also came out of the Moscow meetings mentioned previously.

* Corresponding author.
E-mail address: john.w.norbury@nasa.gov (J.W. Norbury).

https://doi.org/10.1016/j.lssr.2018.05.003
Received 27 February 2018; Received in revised form 17 April 2018; Accepted 12 May 2018
2214-5524/ Published by Elsevier Ltd on behalf of The Committee on Space Research (COSPAR).

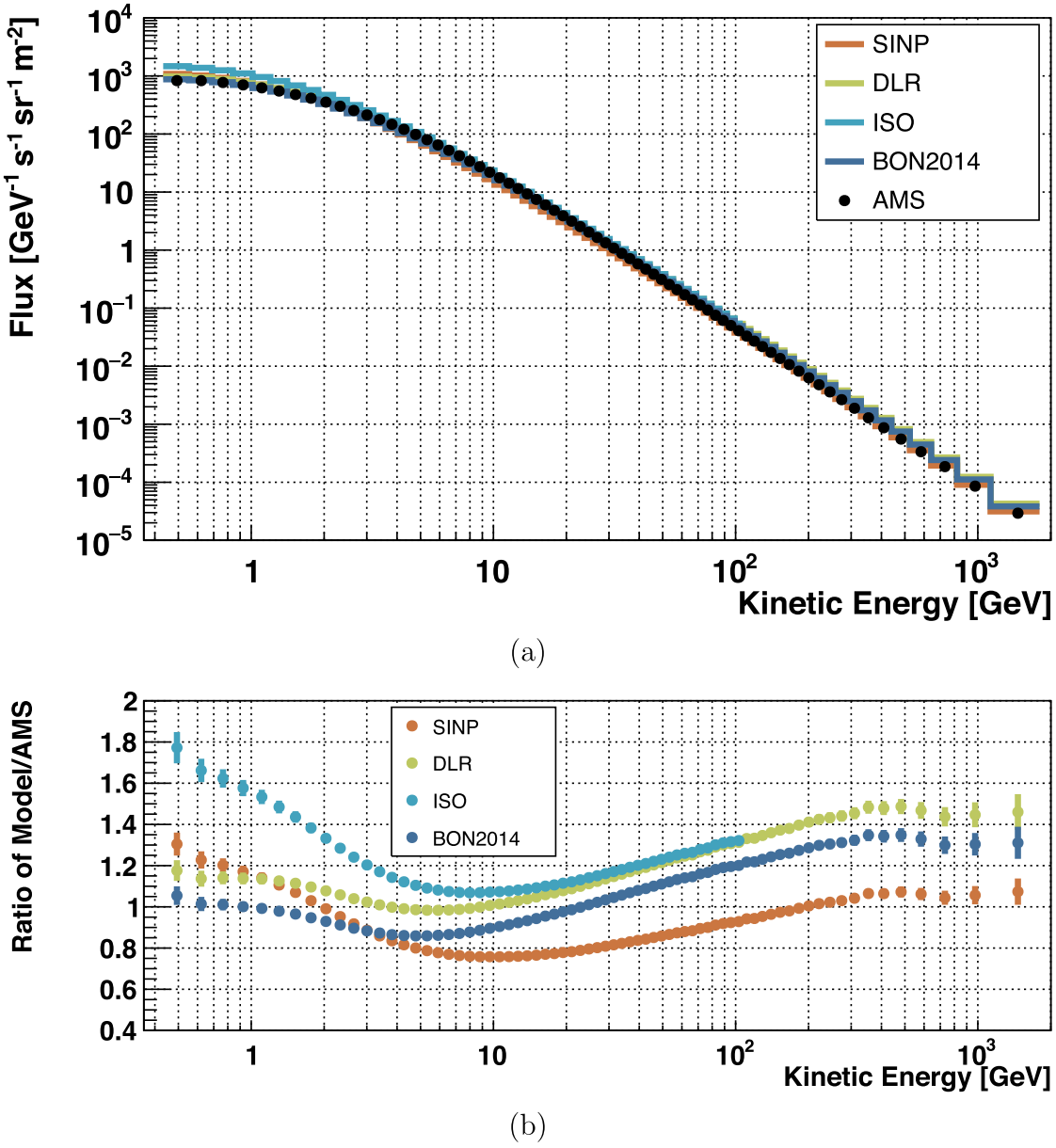

Fig. 1. (a) Models (histograms) compared to AMS Hydrogen flux data (Aguilar et al., 2015) (black circles) integrated from May 19, 2011–November 26, 2013 for the full GCR spectrum. (b) The ratio of each model results divided by AMS data. The error bars include uncertainties from the AMS data only. Ideally, the model ratios would be unity if they agreed perfectly with data.

2. Conversion of AMS data

The AMS data is extensively tabulated in the original references (Aguilar et al., 2015; 2015a; 2016) and is typically given as a function of rigidity R, whereas GCR models are usually a function of kinetic energy T. Even though the conversion is straightforward, it is reviewed here for completeness. Rigidity is defined as

$$R \equiv \frac{|\mathbf{p}|c}{Q} \equiv r_G B \tag{1}$$

which also defines the gyro-radius r_G, where $|\mathbf{p}|$ is the magnitude of the momentum; B is the magnetic field; $Q = Ze$ is the nuclear charge, with Z being the atomic number; e is the electronic charge; and c is the speed of light in vacuum. Units of rigidity are GV (giga-volt) and units of kinetic energy are GeV (giga-electron-volt).

Using $E \equiv T + mc^2$, where m is the particle mass, and $E^2 = (|\mathbf{p}|c)^2 + (mc^2)^2$, gives $E^2 = (RQ)^2 + (mc^2)^2$, so that the rigidity to kinetic energy conversions (x-axis) are

$$T = \sqrt{(RQ)^2 + (mc^2)^2} - mc^2 \tag{2}$$

$$R = \frac{1}{Q}\sqrt{T(T + 2mc^2)} \tag{3}$$

The AMS data is given in terms of differential rigidity flux $\frac{dF}{dR}$ in units of (m^2 sr s GV)$^{-1}$, which needs to be converted to differential kinetic energy flux $\frac{dF}{dT}$ with units (m^2 sr s GeV)$^{-1}$. The (y-axis) conversion from differential rigidity flux to differential kinetic energy flux is given by

$$\frac{dF}{dT} = \frac{dF}{dR}\frac{dR}{dT} = \frac{T + mc^2}{Q\sqrt{T(T + 2mc^2)}}\frac{dF}{dR}. \tag{4}$$

Note that for $T >> mc^2$, the conversion factor $\frac{dR}{dT} \approx \frac{1}{Q}$, so that for a proton ($Q = 1$), one has $\frac{dF}{dT} \approx \frac{dF}{dR}$. In the above equations, note that T is the total kinetic energy and not the kinetic energy/nucleon.

The AMS collaboration uses a different, but equivalent and simpler method to carry out the conversion. The data is given in terms of rigidity bins, with R_{high} and R_{low} defining the upper and lower value of rigidity. The converted kinetic energy bin spans T_{high} to T_{low}. Using these discrete bins, Eq. (4) is written in simpler form as

$$\frac{dF}{dT} = \frac{dF}{dR}\frac{\Delta R}{\Delta T} = \frac{dF}{dR}\frac{R_{high} - R_{low}}{T_{high} - T_{low}}. \quad (5)$$

When carrying out the AMS data conversions in the present work, both Eqs. (4) and (5) were used and, as expected, gave the same results.

3. Calculating the GCR model values

In space, galactic cosmic rays form a continuous energy spectrum. AMS spectra are calculated by defining a set of energy bins and integrating this continuous GCR spectrum within each bin (see original binning, reported in rigidity, in Aguilar et al. (2015) for Hydrogen and Aguilar et al. (2015a) for Helium). To directly compare the models with AMS data, it is most accurate to similarly integrate the GCR spectra produced by each model within the AMS energy bins.

This integration was accomplished by calculating the model spectra for a discrete set of energies, ranging from 100 to 1000 energy bins between approximately 0.01 to 10^8 MeV/n depending on the model (BON2014: 100 bins from 0.009 to 3.94×10^7 MeV/n; DLR: 104 bins from 0.009 to 10^8 MeV/n; ISO: 94 bins from 1 to 1×10^5 MeV/n; SINP: 1000 bins from 0.01 to 2.04×10^6 MeV/n). The discrete energies were interpolated in log space via cubic Lagrangian interpolation to form a continuous spectrum. These interpolated fluxes were then integrated within each AMS energy bin and divided by the bin width to produce the final fluxes for each model, given by:

$$F_{model,i} = \frac{\int_{T_{L,i}}^{T_{L,i}+\Delta T_i} \Phi(T')dT'}{\Delta T_i} \quad (6)$$

where $F_{model,i}$ is the model flux integrated in AMS energy bin i, $T_{L,i}$ is the kinetic energy at the low edge of bin i, ΔT_i is the width of bin i, and $\Phi(T')$ is the interpolated model flux at kinetic energy T'.

Four different GCR models are compared to the recent AMS data. These models are the NASA Badhwar-O'Neill (BON2014) model (O'Neill et al., 2015), the ROSCOSMOS ISO (Nymmik et al., 1992; 1994; 1996; International Standardization Organization ISO, 2004) and SINP (Kuznetsov et al., 2017) models, and the DLR model (Matthia et al., 2013). Current computer codes were used for the BON2014, SINP and DLR models, whereas the ISO model results were obtained by running the code on the SPENVIS[1] web site, which did not provide fluxes for energies above 100 GeV/n. The model details are extensively discussed in the references and will not be repeated here. The recent AMS data includes measurements for the Hydrogen (H) flux (Aguilar et al., 2015) and Helium (He) flux (Aguilar et al., 2015a) integrated over three years between May 19, 2011 and November 26, 2013 and the Boron (B) to Carbon (C) flux ratio (Aguilar et al., 2016) integrated over six years between May 19, 2011 and May 26, 2016.

3.1. Sunspot numbers

Many GCR models, including those considered here, have been calibrated based on sunspot number (SSN) in order to estimate the modulation of GCR flux throughout the solar cycle. In 2015, there was a major revision of the sunspot number count provided by the Solar Influences Data Center (SIDC)[2], designated version 2.

The first major change is related to the 0.6 Zürich scale factor (Clette and Lefèvre, 2016), which originated back in the late 1800s. Until 1893, the reference numbers were produced by Wolf using a small telescope. When his successor A. Wolfer took over, he counted with a larger telescope capable of resolving all existing sunspots, leading to higher counts. Wolf and Wolfer cross calibrated their counts over 17 years and determined that Wolf's counts were lower by a factor 0.6 than the "modern" counts by Wolfer. Rather than adjust Wolf's historical SSN, the 0.6 Zürich scale factor was introduced to adjust the newer counts to the older scale. The version 2 SSN removes this scale factor by multiplying the entire SSN series by 1/0.6.

A second major correction involved the transition between two directors (Waldmeier replacing Brunner) at the Zürich Observatory in 1947, and related modifications in the counting method. The study found that SSN from 1947 onward were systematically higher than those measured before 1947 and large SSN were inflated by up to 17.7%, whereas small SSN were increased by about 1.1% (Clette and Lefèvre, 2016) compared to the measurements before 1947.

Taking these two major corrections into account, the version 2 SSN were increased by 1/0.6 and reduced by approximately 17.7%, resulting in a factor of 1.41 for large SSN.

The GCR models presented in this paper were developed and calibrated using version 1 SSN, which poses a problem for comparison with the AMS B/C ratio, which is integrated up to May 26, 2016 when only version 2 SSN were available. In order to use the models, version 1 SSN values were estimated by multiplying the version 2 SSN by a factor of $1/1.41 = 0.71$. This factor was applied to all sunspot numbers, regardless of level. It was found that this approximation resulted in spectra that were very consistent with those produced using version 1 sunspot numbers.

4. Comparison of models with measurements

The AMS experiment on the ISS is making new high precision measurements of protons and heavy ions from ~400 MeV/n to ~1 TeV/n, which is an energy range that has previously had limited coverage. The GCR models considered here were developed and calibrated before these new results became available to the public; therefore, this study is a unique opportunity for model validation against an independent data set.

In this section, models are plotted alongside data, and numerical comparisons are made for a selection of energy ranges pertinent to space radiation exposure.

4.1. Hydrogen flux

Fig. 1 shows AMS measurements (Aguilar et al., 2015) of the Hydrogen flux (circles) integrated from May 19, 2011 to November 26, 2013 compared to model results (histograms). Fig. 1(a) shows the full GCR spectrum on a log scale and Fig. 1(b) plots the model results divided by data to better interpret the comparison, because the models are hard to distinguish otherwise. The same comparisons are shown again in Fig. 2, but highlighting different portions of the GCR energy spectrum. Fig. 2(a) is plotted on a linear flux scale to focus on the lower energy region, which is important for space radiation protection. Fig. 2(b) shows the flux rescaled by $T^{2.7}$, as is commonly done in high energy astrophysics to highlight the part of the spectrum that is important for distinguishing between models of the origin of cosmic rays. Even though this very high energy region makes a negligible contribution to space radiation exposure, it is interesting nonetheless to compare models.

At lower energies, the ratio (Fig. 1b) and linear (Fig. 2a) plots show that the BON2014 and DLR models are best matched to data. Below ~2 GeV, the BON2014 model reproduces the data closely. The DLR model matches the data very well between ~2–20 GeV. The SINP model first over-predicts and then systematically under-predicts the data across the energy spectrum. The ISO model systematically over-predicts across the entire energy range. It can be seen in Fig. 2(b) that

[1] https://www.spenvis.oma.be/models.php
[2] http://sidc.oma.be/silso/

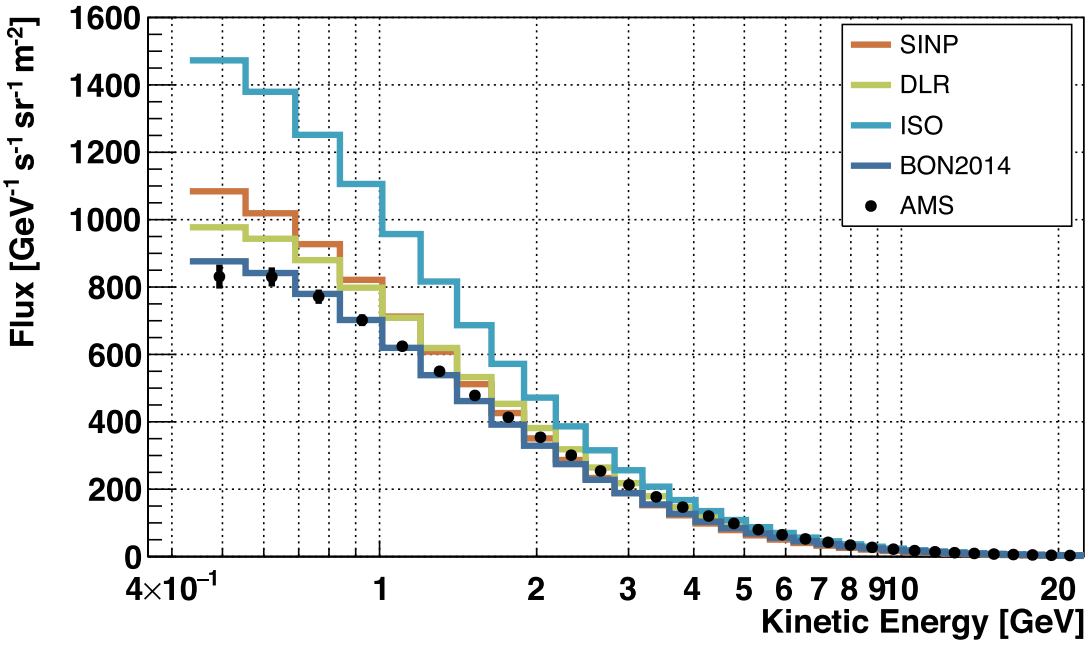

(a)

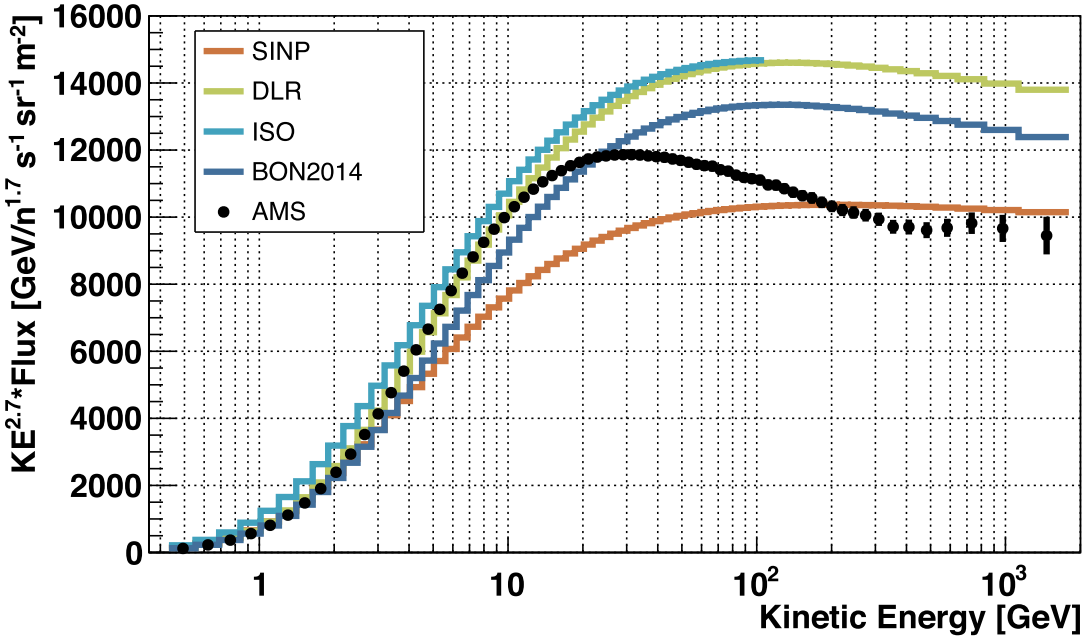

(b)

Fig. 2. The same Hydrogen data (circles) and models (histograms) shown in Fig. 1, but highlighting different parts of the GCR spectrum. (a) Fluxes plotted on a linear scale to emphasize the low energy part of the spectrum. (b) Fluxes scaled by $T^{2.7}$ to better visualize the higher energy part of the spectrum.

all models fail in the very high energy region, particularly above ~30 GeV. Fortunately, as already noted, this region of the spectrum does not significantly impact space radiation exposure.

4.2. Helium flux

Fig. 3 shows AMS measurements (Aguilar et al., 2015a) of the Helium flux (circles) integrated from May 19, 2011 to November 26, 2013 compared to model results (histograms). Fig. 3(a) shows the spectrum over the full energy range, while Fig. 3(b) shows the ratio of model results to data for each model. The low and high energy portions of the He spectrum are highlighted in Fig. 4(a) and (b), respectively.

All of the plots show that the DLR model best reproduces the data across the entire energy spectrum. The SINP model also performs well below ~2 GeV/n, but then under-predicts the remaining part of the He spectrum. The ISO model overestimates the spectrum below ~10 GeV/n, but matches the data fairly well between ~10–100 GeV/n. The BON2014 model produces a spectral shape similar to data, evidenced by the nearly flat ratio seen in Fig. 3(b), but is consistently 12–14% too low across the entire energy range. Fig. 4(b) again shows all models failing in the very high energy region, unimportant for space radiation.

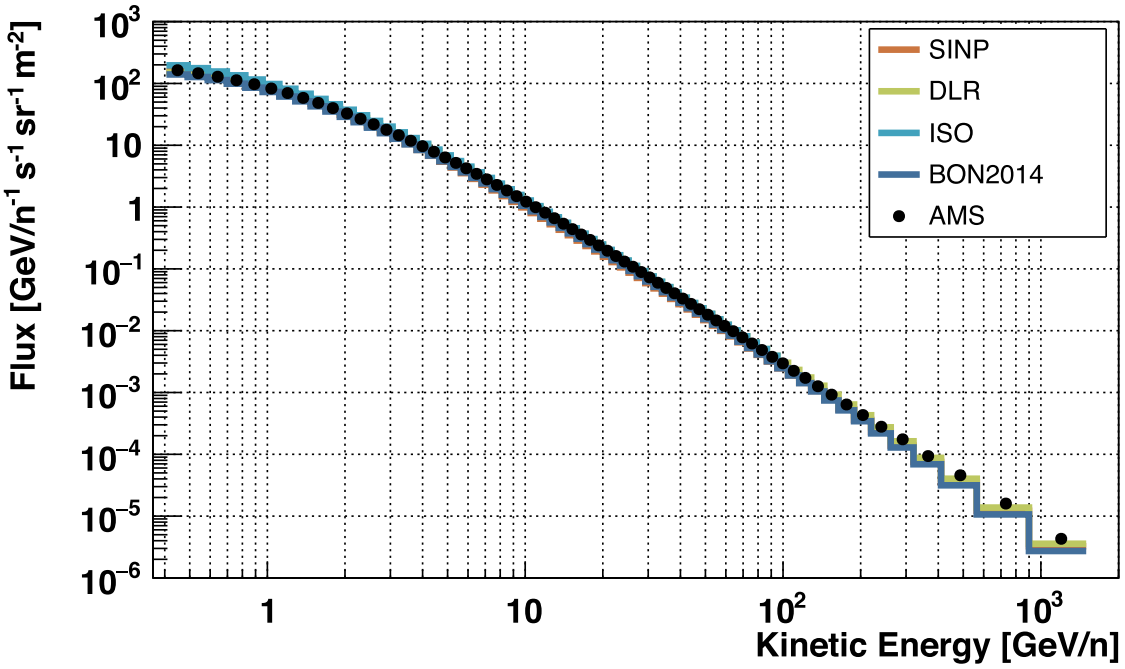

(a)

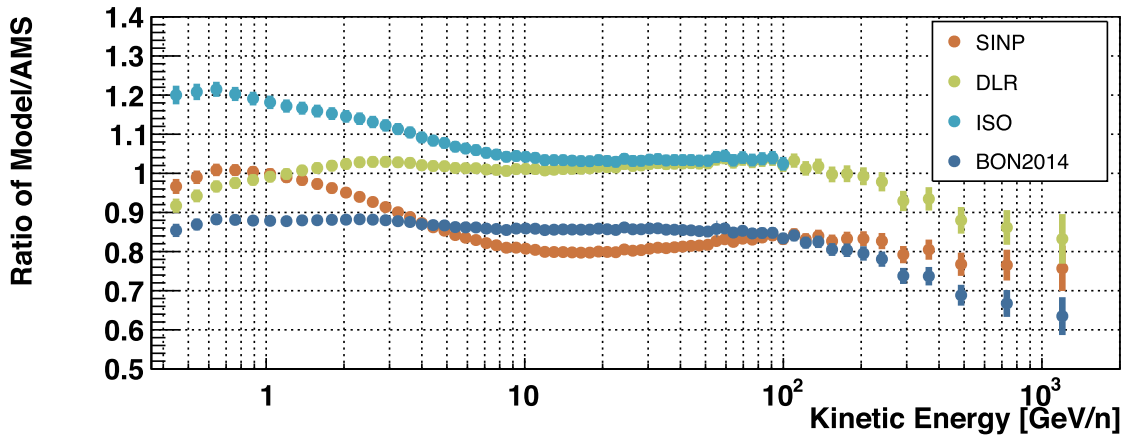

(b)

Fig. 3. (a) Models (histograms) compared to AMS Helium flux data (Aguilar et al., 2015a) (black circles) integrated from May 19, 2011–November 26, 2013 for the full GCR spectrum. (b) The ratio of each model results divided by AMS data. The error bars include uncertainties from the AMS data only.

4.3. Boron-to-carbon (B/C) flux ratio

Astrophysicists typically agree that, whereas Carbon is a primary nucleus reflecting the source abundance, Boron is not created at the source, but is mainly produced from GCR interactions with the interstellar medium. Therefore, the B/C ratio traces the amount of material traversed by GCR nuclei in their journey from the astrophysical source to the AMS detector.

Fig. 5(a) shows AMS measurements (Aguilar et al., 2016) of the B/C flux ratio (circles) integrated from May 19, 2011 to May 26, 2016, compared to model results (histograms). Fig. 5(b) plots the model results divided by data. The ISO and DLR models give comparable results, with slight under-prediction of data at low energy and slight over-prediction at high energy. BON2014 reproduces the data very well, especially below 10 GeV/n where it falls within the measurement uncertainties. In the SINP model, all ion spectra are based on the Helium flux scaled by a constant value, therefore this model cannot be used to study ratios between different heavy ions as it will yield a constant value at all energies.

4.4. Quantification of model differences

The models were compared with the data using two different numerical measures, the absolute relative difference, as done in previous studies by O'Neill et al. (2015) and Slaba et al. (2014), and a χ^2 statistic similar to assessment of GCR models carried out in Mrigakshi et al. (2012).

The absolute relative difference is given by:

$$|Rd| = \frac{1}{N}\sum_{i=1}^{N}\frac{|F_{model,i} - F_{data,i}|}{F_{data,i}} \tag{7}$$

where N is the total number of energy bins and $F_{model,i}$ and $F_{data,i}$ are the flux in energy bin i for model and data, respectively. This sum can also be understood as the average percent difference (when multiplied by 100%) between model and data across the energy range.

It also useful to consider a normalized χ^2 statistic (χ^2/NDF), which

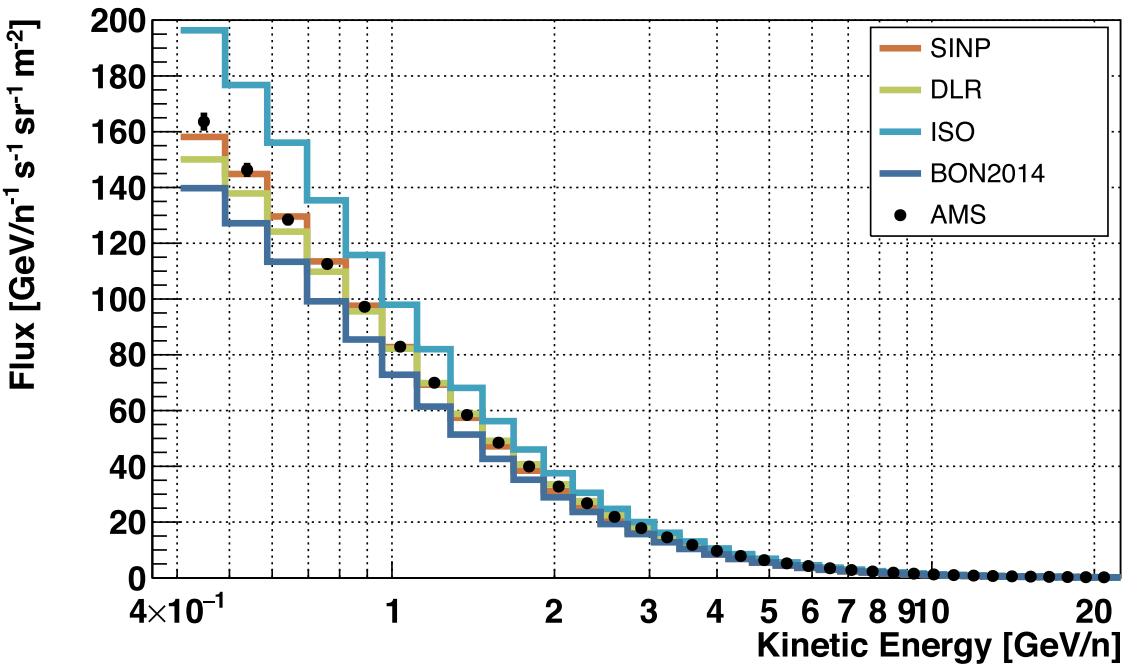

(a)

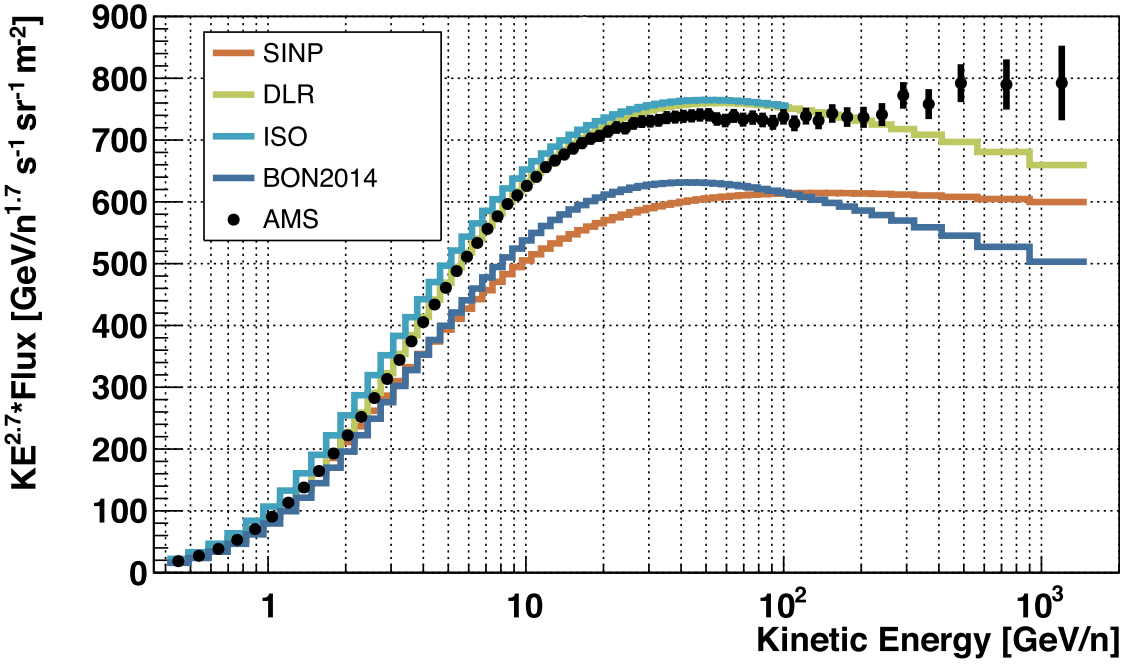

(b)

Fig. 4. The same Helium data (circles) and models (histograms) shown in Fig. 3, but highlighting different parts of the GCR spectrum. (a) Fluxes plotted on a linear scale to emphasize the low energy part of the spectrum. (b) Fluxes scaled by $T^{2.7}$ to better visualize the higher energy part of the spectrum.

incorporates the uncertainties on the data:

$$\frac{\chi^2}{NDF} = \frac{1}{N}\sum_{i=1}^{N}\frac{(F_{model,i} - F_{data,i})^2}{\sigma_i^2} \tag{8}$$

where $F_{model,i}$, $F_{data,i}$, and i are the same as in Eq. (7), and σ_i is the uncertainty on the data in bin i. N is the number of energy bins and also represents the number of degrees of freedom (NDF). The χ^2/NDF values are tabulated in Table 2.

The statistics were calculated for five different energy ranges and tabulated in Tables 1 and 2. Three ranges (< 1.5, 1.5–4.0, and > 4.0 GeV/n) were identified as important energy ranges in the context of space radiation in a series of detailed studies investigating GCR environmental models (Slaba and Blattnig, 2014; 2014a; Slaba et al., 2014). The region < 1.5 GeV/n provides 50% of the effective dose for Al shield thickness of 20g/cm^2, while > 4 GeV/n contributes only 20%. The interval from 4–20 GeV/n was included to discriminate between models that matched the GCR spectra fairly well in that energy range despite deviating significantly at the high end. Lastly, the models were compared across the full spectrum to identify which overall best reproduced the AMS data.

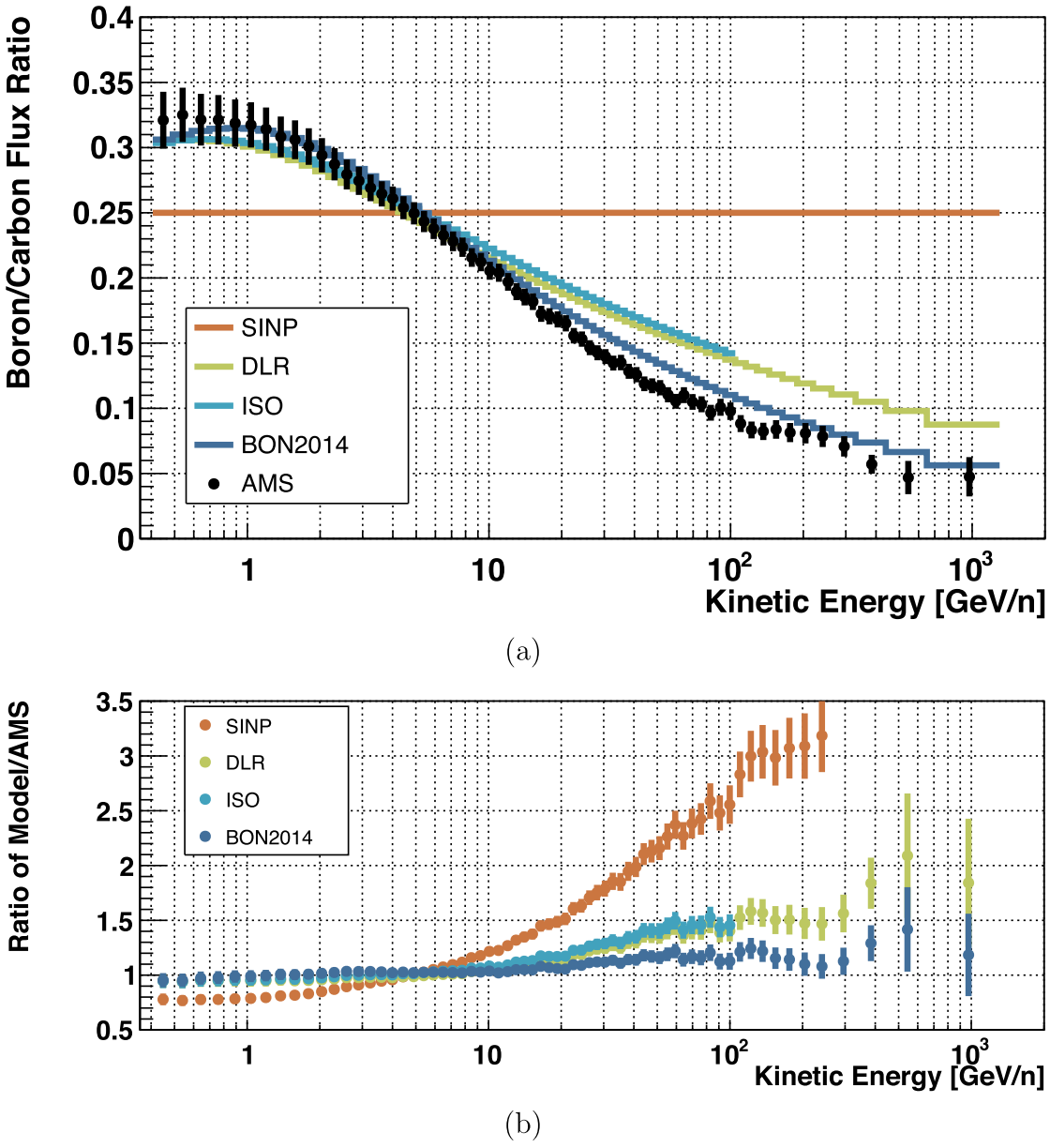

Fig. 5. (a) Models (histograms) compared to the AMS Boron to Carbon ratio (Aguilar et al., 2016) (black circles) integrated from May 19, 2011–May 26, 2016 for the full GCR spectrum. (b) The ratio of each model results divided by AMS data. The error bars include uncertainties from the AMS data only. The SINP ratios for the highest energy bins extend off the plot.

Table 1 lists $|Rd|$ in percent (%) for each model. The lowest values are highlighted in red, indicating the model that best represents the data in each energy range.

The uncertainties in the AMS data are very small, typically a few percent, and the high χ^2/NDF values in Table 2 and large percentage differences in Table 1 clearly indicate that the models are well outside of the data uncertainties, but lower values of χ^2/NDF and $|Rd|$ still indicate whether one model is a better fit to the data relative to another.

According to Tables 1 and 2, the lowest energy part of the H spectrum (< 1.5 GeV) is clearly best represented by the BON2014 model. It differs from data by an average of only 1.8% and the small $\chi^2/NDF < 1$ indicates that the model is within the error bars. At the middle energies between 1.5–4 and 4–20 GeV, the DLR is the closest to data, differing from AMS data on average by $\sim 3-5\%$ with significantly lower χ^2/NDF values than the other models. Considering energies > 4 GeV/n and across the full AMS spectrum, the SINP and BON2014 models have similar $|Rd|$ values, but Fig. 2(a) indicates that SINP generally overestimates the data at the lowest energies (below ~ 3 GeV), while Fig. 2(b) shows that it under-estimates the data at higher energies (above ~ 3 GeV). The χ^2/NDF values in Table 2 indicate that the BON2014 model is the best performer above 4 GeV and across the spectrum.

Tables 1 and 2 show that the AMS He spectrum is best represented by the DLR model, which differs from data on average by less than 3% for all energy ranges. The SINP model does a better job only at the lowest energies < 1.5 GeV/n, where it follows the data closely before systematically underestimating the data.

The B/C ratio is best reproduced by the BON2014 model, except in the range of 1.5–4 GeV/n where the ISO model transitions from underestimating to overestimating the data. Below 4 GeV/n, while BON2014 is best, both DLR and ISO models have $\chi^2/NDF < 1$, indicating that they are also reasonable representations of the data.

For dosimetry studies, the H spectrum would be best represented by the DLR and/or BON2014 model. The former model does an excellent

Table 1
Absolute relative difference ($|Rd|$) in percent (%) between AMS data and the integrated flux calculated from models in selected energy ranges. The lowest values are highlighted in bold typeface. *Note that ISO model results were obtained by running the code on the SPENVIS web site, which did not provide fluxes for energies above 100 GeV/n.

$\|Rd\|$ in % for selected energy ranges (GeV/n)					
Model	< 1.5	1.5–4	> 4	4–20	Full Spectrum
Hydrogen					
SINP	19	8.2	**14**	23	15
DLR	14	**5.3**	22	**2.7**	20
ISO*	61	27	16	8.7	23
BON2014	**1.8**	9.1	16	9.7	**14**
Helium					
SINP	**0.95**	7.5	18	18	15
DLR	2.7	**2.4**	**2.8**	**1.2**	**2.7**
ISO*	19	13	4.1	4.7	7.6
BON2014	12	12	17	14	16
Boron-to-carbon ratio					
SINP	21	11	110	22	86
DLR	5.0	3.1	29	5.3	23
ISO*	4.6	**1.3**	23	8.2	17
BON2014	**2.1**	2.3	**12**	**3.8**	**9.3**

Table 2
Normalized χ^2 for each model compared to AMS data in selected energy ranges. The lowest values are highlighted in bold typeface. *Note that ISO model results were obtained by running the code on the SPENVIS web site, which did not provide fluxes for energies above 100 GeV/n.

χ^2/NDF for Selected Energy Ranges (GeV/n)					
Model	< 1.5	1.5–4	> 4	4–20	Full Spectrum
Hydrogen					
SINP	43.4	44.0	145	317	124
DLR	26.9	**13.7**	248	**7.45**	204
ISO*	474	299	188	47.2	237
BON2014	**0.51**	43	**120**	64.9	**101**
Helium					
SINP	**0.502**	34.5	140	182	110
DLR	3.89	**3.21**	**2.36**	**0.813**	**2.66**
ISO*	151	87.0	9.15	13.3	42.0
BON2014	61.8	75.4	94.3	105	88.0
Boron-to-carbon ratio					
SINP	13.5	7.36	325	56.8	245
DLR	0.761	0.586	26.2	3.90	19.7
ISO*	0.619	**0.165**	33.2	7.69	23.3
BON2014	**0.155**	0.413	**5.00**	**1.42**	**3.81**

job reproducing the AMS He spectrum, while the latter model is the most accurate for the B/C ratio.

5. Summary & conclusions

Widely used GCR models from ROSCOSMOS, ESA, and NASA have been compared with recently published measurements from AMS of cosmic ray Hydrogen, Helium, and the Boron-to-Carbon ratio. This validation study investigated the model accuracy in selected energy ranges pertinent to space radiation exposure. It was found that:

- The AMS H spectrum integrated over three years is best represented by BON2014 over the full energy spectrum and below 1.5 GeV; however, DLR better predicts the data for energies between 1.5–20 GeV. Thus, the best choice of model for H depends on the energy range of interest.
- The AMS He spectrum integrated over three years is best reproduced by the DLR model over all energies, except for < 1.5 GeV/n where the SINP model follows the data closely. The DLR model is also good in this lowest energy range, differing from data by only 2.7% on average.
- The AMS B/C ratio integrated over six years is very well matched by BON2014 across the spectrum.

It should be noted that all models fail to duplicate the high energy parts of the AMS spectra, particularly in the case of Hydrogen. However, this energy region makes a negligible contribution to space radiation.

This analysis compared GCR models to AMS data integrated over significant portions of the solar cycle. These three or six year integration times were averaged over the time-dependent effects of solar modulation. It is also important to understand how well models replicate solar modulation on shorter timescales. When high time resolution AMS data of H and heavy ions becomes available, it will be imperative and enlightening to repeat this analysis to test the accuracy of GCR models with time.

Acknowledgments

We thank Claudio Corti and Veronica Bindi for useful discussions and correspondence, Daniel Matthiä for providing data updates for input into the DLR code, and Nikolay Kuznetsov for his valuable insights regarding the SINP model. This work was supported by the Advanced Exploration Systems (AES) Division under the Human Exploration and Operations Mission Directorate of NASA.

References

Aguilar, M., et al., 2015. Precision measurement of the proton flux in primary cosmic rays from rigidity 1 GV to 1.8 TV with the alpha magnetic spectrometer on the international space station. Phys. Rev. Lett. 114, 171103.
Aguilar, M., et al., 2015a. Precision measurement of the helium flux in primary cosmic rays of rigidities 1.9 GV to 3 TV with the alpha magnetic spectrometer on the international space station. Phys. Rev. Lett. 115, 211101.
Aguilar, M., et al., 2016. Precision measurement of the boron to carbon flux ratio in cosmic rays from 1.9 GV to 2.6 TV with the alpha magnetic spectrometer on the international space station. Phys. Rev. Lett. 117, 231102.
Clette, F., Lefèvre, L., 2016. The new sunspot number: assembling all corrections. Solar Phys. 291, 2629–2651.
International Standardization Organization (ISO), 2004. Space Environment (Natural and Artificial) - Galactic Cosmic Ray Model. ISO 15390.
Kuznetsov, N.V., Popova, H., Panasyuk, M.I., 2017. Empirical model of long-time variations of galactic cosmic ray particle fluxes. J. Geophys. Res. Space Phys. 115, 1463–1472.
Matthia, D., Berger, T., Mrigakshi, A.I., Reitz, G., 2013. A ready-to-use galactic cosmic ray model. Adv. Space Res. 51, 329–338.
Mrigakshi, A.I., Matthia, D., Berger, T., Reitz, G., 2012. Assessment of galactic cosmic ray models. J. Geophys. Res. 117, A08109.
Norbury, J.W., Slaba, T.C., Sobolevsky, N., Reddell, B., 2017. Comparing HZETRN, SHIELD, FLUKA and GEANT transport codes. Life Sci. Space Res. 14, 64–73.
Norbury, J.W., Sobolevsky, N., Werneth, C.M., 2018. SHIELD comparisons to pion cross section parameterizations for space radiation codes. Nucl. Instr. Meth. Phys. Res. B 418, 13–17.
Nymmik, R.A., Panasyuk, M.I., Pervaya, T.I., Suslov, A.A., 1992. A model of galactic cosmic ray fluxes. Nucl. Tracks Radiat. Meas. 20, 427–429.
Nymmik, R.A., Panasyuk, M.I., Pervaya, T.I., Suslov, A.A., 1994. An analytical model describing dynamics of galactic cosmic ray heavy particles. Adv. Space Res. 14, (10) 759–(10)763.
Nymmik, R.A., Panasyuk, M.I., Suslov, A.A., 1996. Galactic cosmic ray flux simulation and prediction. Adv. Space Res. 17, (2)19–(2)30.
O'Neill, P.M., Golge, S., Slaba, T.C., 2015. Badhwar - O'Neill 2014 Galactic Cosmic Ray Flux Model Description. NASA Technical Paper 2015–218569.
Slaba, T.C., Blattnig, S.R., 2014. GCR environmental models I: sensitivity analysis for GCR environments. Space Weather 12, 217–224.
Slaba, T.C., Blattnig, S.R., 2014a. GCR environmental models II: uncertainty propagation methods for GCR environments. Space Weather 12, 225–232.
Slaba, T.C., Xu, X., Blattnig, S.R., Norman, R.B., 2014. GCR environmental models III: GCR model validation and propagated uncertainties in effective dose. Space Weather 12, 233–245.